The αA-Crystallin R116C Mutant Has a Higher Affinity for Forming Heteroaggregates with αB-Crystallin†

Sibes Bera and Edathara C. Abraham*

Department of Biochemistry and Molecular Biology, University of Arkansas for Medical Sciences, Little Rock, Arkansas 72205

Received May 17, 2001; Revised Manuscript Received September 12, 2001

ABSTRACT: An autosomal dominant congenital cataract in humans is associated with mutation of Arg-116 to Cys in αA-crystallin (αA-R116C). The chaperone activity and biophysical properties of reconstituted α-crystallin from different proportions of wild-type αB-crystallin (αB-wt) and αA-R116C-crystallin were studied by gel permeation chromatography, SDS−polyacrylamide gel electrophoresis, and fluorescence and circular dichroism spectroscopy and compared with those of reconstituted α-crystallin from αB-wt and wild-type αA-crystallin (αA-wt). The reconstituted α-crystallin containing αA-R116C and αB-wt had a higher molecular mass, a higher thermal sensitivity to exposition of Trp side chains, fewer available hydrophobic surfaces, and lower chaperone activity than the α-crystallin containing αA-wt and αB-wt. The secondary structure exhibited very small changes, whereas the tertiary structure was distinctly different for α-crystallin formed from αA-R116C and αB-wt. Most importantly, subunit exchange studies by fluorescence resonance energy transfer showed that αA-R116C forms heteroaggregates faster than αA-wt with αB-wt, and the reconstituted α-crystallins were true heteroaggregates of two interacting subunits. These findings suggest that the molecular basis for the congenital cataract with the αA-R116C mutation is the formation of highly oligomerized heteroaggregates of α-crystallin with modified structure. However, contrary to the earlier conclusions based on the studies of homoaggregates, the loss in chaperone activity of the heteroaggragates having αA-R116C does not appear to be large enough to become the main factor in initiating cataract development in the affected individuals.

α-Crystallin is the major multimeric protein of the mammalian eye lens. It is composed of two types of polypeptide chains (subunits), αA and αB chains, which are highly homologous and conserved (*1*−*3*). These are believed to be present in the protein in an approximately 3:1 to 1:1 αA:αB ratio depending on the age (*4*). Being the largest in size among the crystallins having a molecular mass in the 300−800 kDa range and also being highly abundant in the lens, α-crystallin is believed to play a dominant role in maintaining the transparency of the lens and its impairment during cataractogenesis. Apart from its conventional structural role in the lens, additional importance has been attached to this protein because of the discovery that α-crystallin functions in the eye lens as a molecular chaperone (*5*). For many years it was believed that the expression of α-crystallins was restricted to the ocular lens. In 1989, αB-crystallin was found in tissues other than lens, i.e., in heart, brain, spleen, striated muscle, kidney, etc. (*6*−*8*). In 1991, Kato et al. detected very small amounts of αA-crystallin in rat spleen (*9*). αB-Crystallin has been known to be associated with various neurodegenerative diseases, including Creuzfeldt-Jacob disease, Pick's disease, and Alzheimer's disease, and muscle diseases (*10*−*13*).

Congenital cataracts are a common cause of blindness in infants. One type of such a cataract is known to be associated with mutation of Arg-116 to a Cys residue in the αA-crystallin subunit (*14*). In our previous studies, we reported that the αA-R116C homoaggregate exists as a highly oligomerized protein with perturbed secondary and tertiary structure and decreased chaperone activity (*15*, *16*). However, it has not been shown how this mutation in the αA subunit affects the formation of α-crystallin heteroaggregates with the αB subunit and whether this mutation causes structural and functional changes in α-crystallin. Since the ratio of αA to αB in α-crystallin varies from 3:1 to 1:1, depending on the age, we reconstituted α-crystallin heteroaggregates from αA-wt and αB-wt and from αA-R116C and αB-wt using the two extreme ratios of 3:1 and 1:1 which demonstrated that the reconstituted α-crystallin from αA-R116C and αB-wt has relatively larger molecular size, altered tertiary structure, and decreased chaperone activity as compared to reconstituted αA-wt and αB-wt. Moreover, subunit exchange studies strongly supported the formation of heteroaggregates in which αA-R116C interacts with αB at a faster rate than αA-wt.

EXPERIMENTAL PROCEDURES

Materials. N-(1-Pyrene)maleimide (PM),[1] 7-(dimethylamino)cumarin-4-acetic acid, succinimidyl ester (DMACA), lucifer yellow iodoacetamide (LYI), and 4-acetamido-4′-isothiocyanatostilbene-2,2′-disulfonic acid (AIAS) were purchased from Molecular Probes (Eugene, OR). 2-(*p*-Toluidino)-

† This work was supported by Grants EY 11352 and EY 07394 from the National Institutes of Health.

* To whom correspondence should be addressed: Edathara C. Abraham, Department of Biochemistry and Molecular Biology, University of Arkansas for Medical Sciences, 4301 W. Markham St., Slot 516, Little Rock, AR 72205. Telephone: (501) 526-6088. Fax: (501) 686-8169. E-mail: abrahamedatharac@uams.edu.

10.1021/bi011010v CCC: $22.00
Published on Web 12/11/2001

naphthalene-6-sulfonic acid (TNS) and guanidine hydrochloride (GdnHCl) were obtained from Sigma Chemicals.

Cloning, Expression, and Purification of Recombinant αA-wt and αB-wt and Mutant αA-Crystallin. Cloning and subsequent subcloning into the pET-23d(+) (Novagen) expression vector of rat αA-crystallin (*15*) and αB-crystallin (*17*, *18*) were described previously. BL21(DE3) pLysS *Escherichia coli* cells (Novagen) harboring the pET-23d(+) αA-crystallin, αA-S142C/R116C (αA-R116C), and αB-crystallin constructs were grown in 500 mL of LB to a cell density of ≈0.6 at 600 nm and induced with 0.5 mM isopropyl thio-*β*-D-galactoside for 3 h. Cells were harvested by centrifugation at 4000*g* for 10 min, resuspended in 10 mL of lysis buffer [20 mM Tris (pH 7.4), 1 mM EDTA, 4 *μ*g/mL pepstatin A, 4 *μ*g/mL aprotinin, and 0.1 M PMSF]. After three freeze−thaw cycles, 800 units of DNase (Sigma) and 5 units of RNase (Sigma) and 10 mM $MgCl_2$ were added to the cell lysate, and incubation was carried out at room temperature on the nutator for 3 h with subsequent centrifugation at 28000*g* for 45 min. The protein was filtered through a 0.2 *μ*m filter and loaded onto a Sephacryl S-300 HR molecular sieve column (120 cm × 2.6 cm). SDS−PAGE was used to examine the fractions; those containing more than 95% wild-type and mutant crystallin were pooled and concentrated by ultrafiltration in an Amicon stirred cell.

Reconstitution of α-Crystallin Heteroaggregates from αB-wt, αA-wt, and the αA-R116C Mutant and Determination of Oligomeric Sizes. For faster reconstitution of heteroaggregates, we followed the process of dissociation and reassociation. Purified protein solutions of a concentration of ∼4 mg/mL were denatured with 4 M GdnHCl for 6 h under a nitrogen atmosphere at room temperature. The α-crystallin was reconstituted by mixing different proportions (1:1 and 3:1 αA:αB, keeping a constant protein concentration of 4 mg/mL) of αA-wt or αA-R116C and αB-wt followed by a slow dialysis process. Purification of the reconstituted protein was done by gel permeation chromatography on a Sephacryl S300 HR column (100 cm × 1.6 cm). A peristaltic pump maintained a constant flow rate of 30 mL/h. Approximately 8 mg of protein in 2 mL of 50 mM phosphate buffer (pH 7.4) was applied to the column. The elution was performed with the same buffer, and fractions of 1 mL were collected and monitored at 280 nm. High-molecular mass standards (Sigma) were used to calibrate the column. Molecular masses (*M*) were determined from a plot of log *M* versus V_e/V_o (where V_e is the elution volume and V_o is the void volume).

SDS−PAGE of Reconstituted α-Crystallin and Determination of Subunit Ratios from Densitometric Scanning. SDS−PAGE was performed using a 12% separating gel and 4% stacking gel under reducing conditions, according to the method of Laemmli (*19*). The gel was stained with Coomassie brilliant blue R-250. The relative levels of αA and αB subunits in the reconstituted α-crystallin were determined by densitometric scanning of the stained protein bands on the gel at 600 nm using the dual-wavelength flying spot scanner (Shimadzu CS 9000) and estimating the relative areas under the scan curves.

Circular Dichroism (CD) Measurements. To investigate the conformation of the reconstituted α-crystallins, CD spectra were measured with a Jasco spectropolarimeter (model J710) at room temperature. Protein concentrations of 1.0 and 0.1 mg/mL in 50 mM potassium phosphate buffer (pH 7.4) were used for recording the near- and far-UV CD spectra, with 1 cm and 0.1 cm path length quartz cells, respectively. The reported spectra are the average of five scans, which were smoothed, and corrected for buffer blanks. CD data were expressed as molar ellipticity in degrees per square centimeter per decimole, with 115 as the mean residue molecular weight. Secondary structure parameters were estimated by the computer program PROSEC.

Labeling of Recombinant αA-wt, αB-wt, and αA-Crystallin Mutants with Different Fluorescence Probes. To 1 mL of a protein solution (3 mg/mL) in 20 mM MOPS buffer containing 100 mM NaCl (pH 7.9) was added a 10-fold excess of solid AIAS, and the reaction was allowed to proceed for ∼16 h at room temperature (25 °C) in the dark. The unreacted reagent was then separated from the fluorescently labeled protein on a Sephadex G-25 column equilibrated with 50 mM phosphate buffer (pH 7.4). LYI-, PM-, and DMACA-labeled protein was prepared similarly in 50 mM phosphate buffer with a 20-fold molar excess of the reagent. In the case of PM and DMACA, reagents were dissolved in DMSO. The extent of labeling was determined spectrophotometrically using molar extinction coefficients of 40 000 mol^{-1} cm^{-1} at 338 nm for PM, 22 000 mol^{-1} cm^{-1} at 376 nm for DMACA, 47 000 mol^{-1} cm^{-1} at 336 nm for AIAS, and 11 000 mol^{-1} cm^{-1} at 426 nm for LYI, with a corrected protein concentration (corrected for the contribution of the dye at 280 nm).

Heat-Induced Exposure of Trp Side Chains in Reconstituted α-Crystallin. The tryptophan fluorescence of the protein solutions (0.1 mg/mL) in 50 mM phosphate buffer (pH 7.4) at 25−60 °C was measured with an excitation wavelength of 295 nm and an emission range of 310−400 nm. Temperature-dependent studies have been carried out using a water-jacketed cell holder with a constant-temperature water bath on a Shimadzu spectrofluorometer (model RF-5301PC). Each reading was taken after incubation for 10 min prior to reaching that temperature. Emission maxima (nanometers) were then plotted against temperature.

TNS [2-(p-Toluidino)naphthalene-6-sulfonic Acid] Binding Studies. The fluorescence of TNS in the presence of reconstituted α-crystallins was measured using an excitation wavelength of 320 nm and an emission range of 350−550 nm. All measurements were performed in 50 mM phosphate buffer (pH 7.4). Typically, to 1 mL of a protein (0.1 mg/mL) solution was added 5 *μ*L of 20 mM TNS in DMSO, and the mixture was incubated for 2 h at 37 °C.

Reconstitution of Heteroaggregates Containing Fluorescent Label and Fluorescence Resonance Energy Transfer (FRET) Studies. Labeled homoaggregate proteins (αA-PM, αA-R116C-PM, and αB-DMACA) were dissociated to subunits using 4 M GdnHCl (final concentration). FRET was employed to determine the formation of heteroaggregates by mixing αA- and αB-crystallin subunits with subsequent dilution of GdnHCl. The exchange reaction was initiated by mixing a 3:1 ratio of αA-crystallin to αB-crystallin with a

[1] Abbreviations: PM, *N*-(1-pyrene)maleimide; DMACA, 7-(dimethylamino)cumarin-4-acetic acid, succinimidyl ester; LYI, lucifer yellow iodoacetamide; AIAS, 4-acetamido-4′-isothiocyanatostilbene-2,2′-disulfonic acid; TNS, 2-(*p*-toluidino)naphthalene-6-sulfonic acid; GdnHCl, guanidine hydrochloride; ADH, alcohol dehydrogenase; FRET, fluorescence resonance energy transfer.

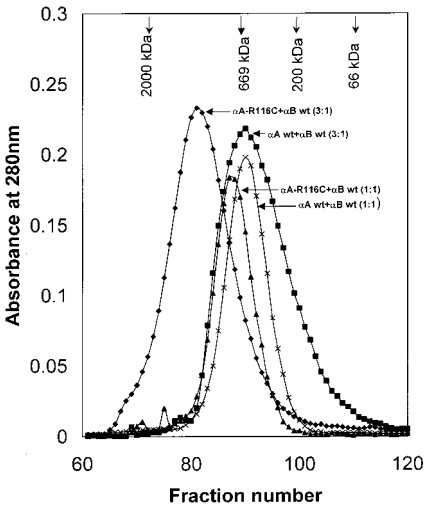

FIGURE 1: Comparison of the size distribution of reconstituted α-crystallins. Purification and determination of the molecular masses of reconstituted α-crystallins were achieved by size-exclusion chromatography on a Sephacryl S-300HR column. The numbers on the top refer to the masses of the molecular mass protein standards from which molecular masses of the reconstituted α-crystallins have been determined.

final protein concentration being 1 mg/mL. After each dilution, the mixture was thoroughly mixed and left to incubate for 10 min (such an incubation was found to be sufficient to establish equilibrium). The emission spectra of the mixture excited at 338 nm (for donor fluorophore, emission maxima at 376 nm) were recorded in the range of 360−520 nm, and the readings were corrected for dilution (data not shown). The increase in fluorescence intensity at 468 nm due to energy transfer from the donor molecule (αA-PM/αA-R116C-PM, emission maxima at 376 nm) to the acceptor molecule (αB-DMACA, absorption maxima at a wavelength of 376 nm and emission maxima at a wavelength of 468 nm) was then plotted versus the GdnHCl concentration. For measurements of the rate of subunit exchange, the LYI-labeled αA-homoaggregate was mixed with an AIAS-labeled αB-homoaggregate (3:1 ratio) to form heteroaggregates (in the absence of GdnHCl). Time-dependent emission spectra were obtained at an excitation wavelength of 336 nm, and the decrease in AIAS emission intensity at 415 nm and increase in LYI emission intensity at 515 nm were determined. The rate of subunit exchange was determined by nonlinear regression analysis of the data.

Chaperone Activity of Reconstituted α*-Crystallin*. The denaturation and aggregation of alcohol dehydrogenase (ADH) in the absence and in the presence of reconstituted α-crystallins were assessed in a Shimadzu UV-2401PC spectrophotometer equipped with a temperature-regulated cell holder. α-Crystallin:ADH ratios of 1:2 and 1:10 were used to determine chaperone-like activity. ADH (250 μg/mL) was denatured using 10 mM EDTA at 37 ± 1 °C, and light scattering was monitored at 360 nm.

RESULTS

Molecular Masses and Subunit Ratios of Reconstituted α*-Crystallins.* To purify the major population of reconstituted heteroaggregates α-crystallin from the mixture, analytical size-exclusion chromatography was performed at room temperature. The size of reconstituted α-crystallin (major peak) from αA-R116C-crystallin and αB-wt-crystallin (1:1 mixing) was ∼725 kDa, whereas for αA-wt and αB-wt at the same ratio, it was 610 kDa (Figure 1). But when the subunits were mixed in a 3:1 ratio (αA:αB), the sizes were 1340 and 610 kDa, respectively, for αA-R116C with αB-wt and αA-wt with αB-wt. The reconstituted α-crystallin from αA-R116C with αB-wt for both ratios is larger than the reconstituted α-crystallin from αA-wt with αB-wt. To determine the actual subunit ratios in the reconstituted α-crystallin, SDS−PAGE (figure not shown) was carried out followed by densitometric scanning of the gel. αA:αB ratios of 1:1 and 1:1 for 1:1 mixing and 3:1.4 and 3:2.4 for 3:1 mixing were found for αA-wt with αB-wt and αA-R116C with αB-wt, respectively.

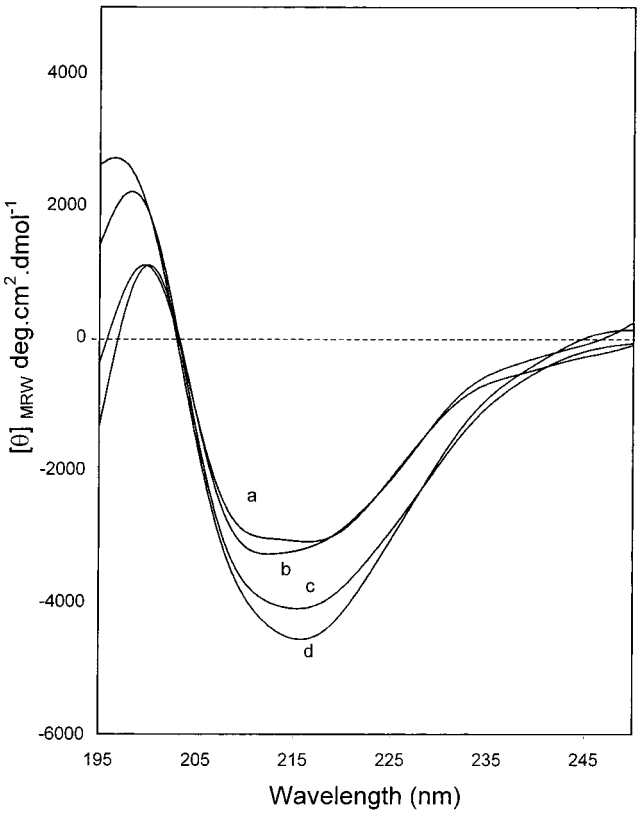

FIGURE 2: Far-UV CD spectra of reconstituted α-crystallin in 50 mM phosphate buffer (pH 7.4). The protein concentration for far-UV CD measurements was ∼0.1 mg/mL, and a cylindrical quartz cell with a path length of 1 mm was used: (a) αA-wt and αB-wt (1:1), (b) αA-R116C and αB-wt (1:1), (c) αA-wt and αB-wt (3:1.4), and (d) αA-R116C and αB-wt (3:2.4).

Structural Studies of Reconstituted α*-Crystallins.* Far- and near-UV CD spectra are shown in Figures 2 and 3, respectively. When secondary structures (Figure 2) of the reconstituted α-crystallin from αA-R116C with αB-wt and αA-wt with αB-wt were analyzed in detail, the former showing very small difference in structural components (a nearly 2% increase in α-helix content and a 2% decrease in β-turn content) regardless of their reconstitution ratios. Tertiary structural differences in the intensities mainly in the 265−285 nm regions for reconstituted αA-R116C with αB-wt were found from near-UV CD spectra (Figure 3). To see the tertiary structural changes upon formation of heteroaggregates, we scanned immediately mixed (not reconstituted) αA-wt with αA-R116C and αB-crystallin with the same ratios that were used for the reconstituted α-crystallin at room

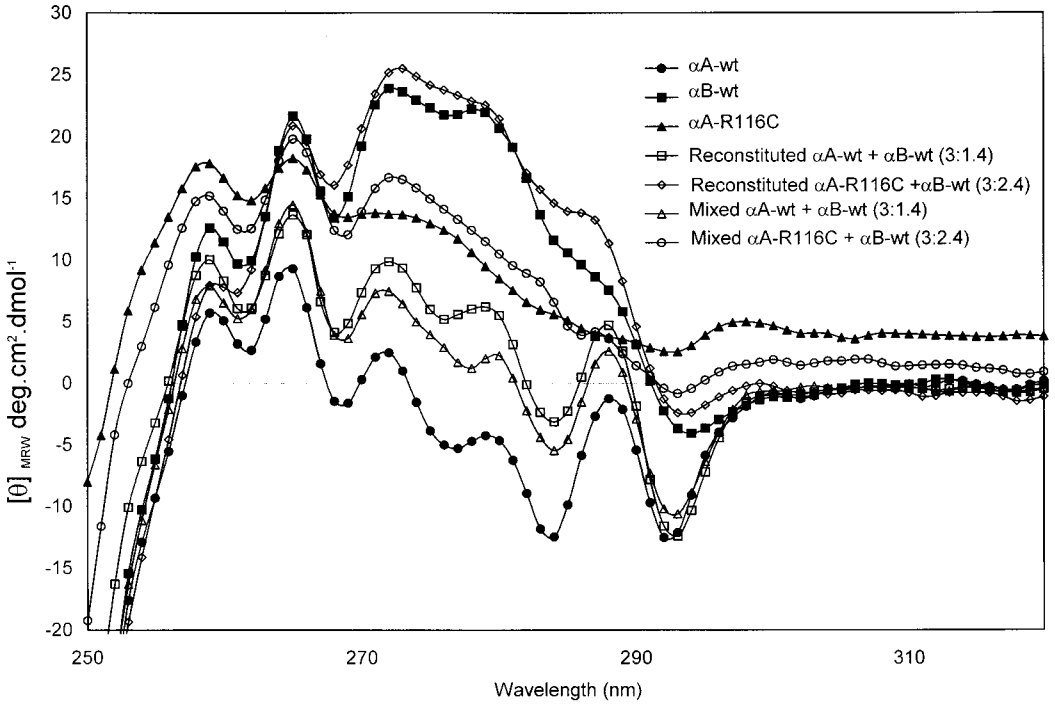

FIGURE 3: Near-UV CD spectra of reconstituted α-crystallin as well as homopolymers and a simple mixture of αA-wt or αA-R116C with αB-wt at 3:1.4 and 3:2.4 ratios in 50 mM phosphate buffer (pH 7.4). The protein concentration for near-UV CD measurements was ~1 mg/mL, and a cylindrical quartz cell with a path length of 1 cm was used. Five scans were recorded and averaged for each sample, corrected for the cell blank, and smoothed for eliminating background noises. The ellipticity is expressed in degrees per square centimeter per decimole, and the mean residue molecular weight was taken to be 115.

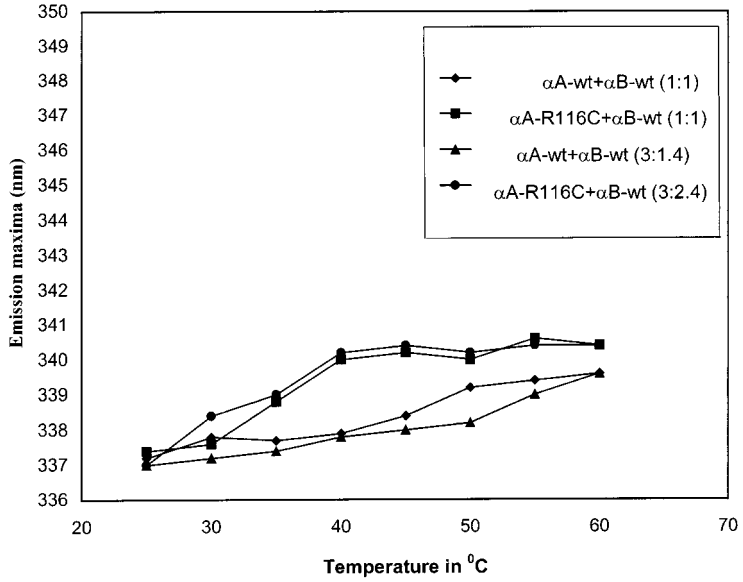

FIGURE 4: Heat-induced exposure of Trp in reconstituted α-crystallins. Trp emission maxima (excitation at 295 nm) of reconstituted α-crystallins [0.1 mg/mL in 50 mM phosphate buffer (pH 7.4)] have been plotted vs temperature.

temperature. The increase in intensities between reconstituted and mixed α-crystallin was more for the reconstituted α-crystallin from αA-R116C and αB-wt than for reconstituted α-crystallin from αA-wt and αB-wt (Figure 3).

Thermally Induced Exposure of Trp Side Chains of Reconstituted α-Crystallins. The exposure of Trp residues in the reconstituted α-crystallins was determined by monitoring Trp emission maxima in the temperature range of 25−60 °C (Figure 4). When the temperature was increased from 25 to 40 °C, the Trp emission maxima red shifted from 337.2 to 340 nm in the case of the reconstituted α-crystallin from αA-R116C with αB-wt, while reconstituted α-crystallin from αA-wt with αB-wt showed a shift from only 337.2 to 337.8 nm. The data show that the microenvironments of Trp residues of the reconstituted crystallin from αA-R116C with αB-wt are thermally sensitive.

Relative Hydrophobicity of the Reconstituted α-Crystallins. TNS is a hydrophobic molecule that becomes highly fluorescent upon binding to protein hydrophobic sites (*20*, *21*). Figure 5 shows the fluorescence spectra of TNS bound with different reconstituted α-crystallins. A highest relative intensity was found for reconstituted α-crystallin with a 1:1

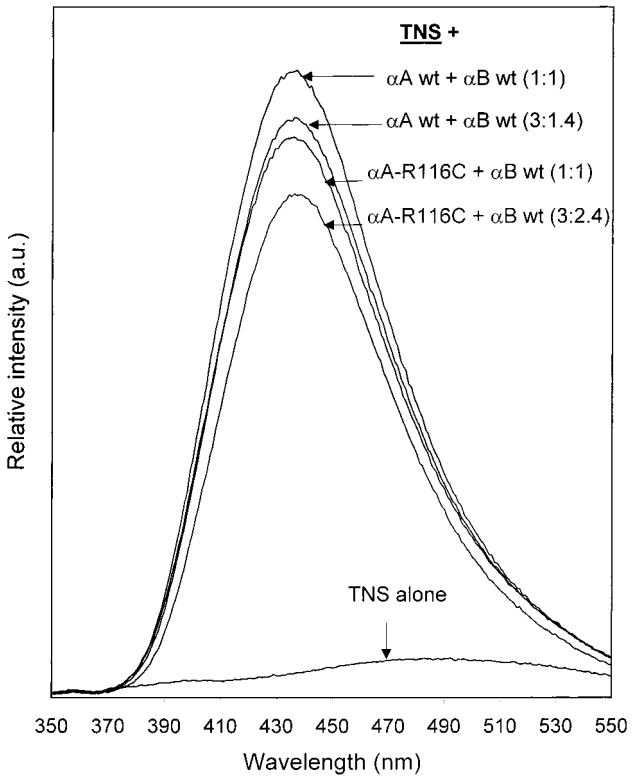

FIGURE 5: TNS interaction with reconstituted α-crystallins. One milliliter of protein (0.1 mg/mL) in 50 mM phosphate buffer was incubated with 5 μL of 20 mM TNS in DMSO for 2 h. Fluorescence spectra of the TNS-bound form were recorded using an excitation wavelength of 320 nm and an emission range of 350−550 nm.

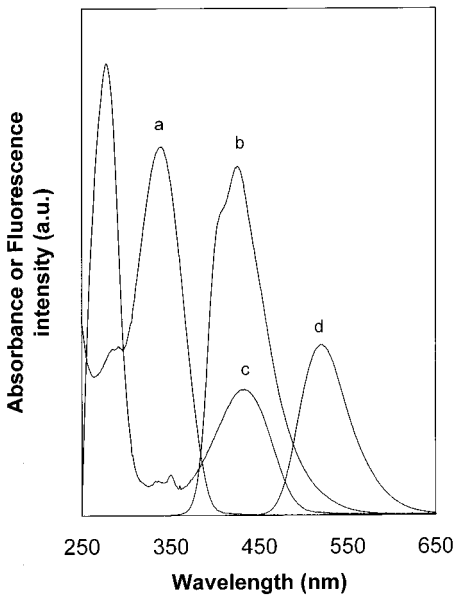

FIGURE 6: Spectral properties of AIAS-labeled and LYI-labeled crystallin. Absorption (a and c) and fluorescence emission (b and d) spectra of αB-AIAS (a and b) and αA-R116C-LYI (c and d) labeled protein. The emission maxima for AIAS-labeled protein excited at 336 nm and LYI-labeled protein excited at 426 nm are 425 and 515 nm, respectively. The protein:fluorophore molar ratios are ∼1:1 and ∼1:2 for αB-wt to fluorophore and αA-R116C to fluorophore, respectively.

αA-wt:αB-wt ratio, followed by a 3:1.4 αA-wt:αB-wt ratio and a 1:1 αA-R116C:αB-wt ratio, and was lowest for a 3:2.4 αA-R116C:αB-wt ratio. Therefore, the available hydrophobic surface is in the following order: 1:1 αA-wt:αB-wt > 3:1.4 αA-wt:αB-wt > 1:1 αA-R116C:αB-wt > 3:2.4 αA-R116C: αB-wt.

Labeling of αA-wt, αA-R116C, and αB-wt with Fluorescent Probes. Recombinant rat αA-wt contains a single cysteine residue, and αA-R116C has three cysteine residues. Labeling of PM revealed that there is on average 1 mol of fluorophore/mol of αA-wt and 2 mol of fluorophore/mol of αA-R116C. DMACA and AIAS are commonly known to be amine specific reagents. Approximately 1 mol of DMACA and AIAS was attached to the αB-wt protein. Likewise, 1 mol of LYI was attached to αA-wt, and 2 mol of LYI was attached to αA-R116C. Figure 6 shows the emission maxima of AIAS-labeled αB-crystallin excited at 336 nm and LYI-labeled αA-R116C excited at 426 nm with emission maxima around 422 and 516 nm, respectively. The significant overlap of the emission spectrum of the AIAS fluorophore with the absorption spectrum of the LYI fluorophore results in FRET when they come closer to each other.

Rate Constant of Subunit Exchange Determined by FRET of Mixing Labeled Subunits. We demonstrated the formation of heteroaggregates in which the subunits are truly interacting by doing a FRET study at room temperature (25 °C). When PM-labeled αA-wt or αA-R116C was mixed with DMACA-labeled αB-wt in a 3:1 ratio in the presence of 4 M GdnHCl, no energy transfer could take place because the subunits were far apart due to dissociation (*22*). But, with decreasing GdnHCl concentrations, fluorophore-labeled monomers come closer to each other (reassociation) to form heteroaggregates. As a result, FRET takes place, the fluorescence emission intensity at 376 nm of the donor molecule (PM-labeled αA-wt or αA-R116C) decreases, and the fluorescence emission intensity at 468 nm of the acceptor molecule (αB-DMACA) increases. The emission intensity (F/F_0) at 468 nm (corrected) was plotted versus the decreasing concentration of GdnHCl (Figure 7). The subunit exchange between αA-R116C and αB-wt was faster than that between αA-wt and αB-wt. The rate of subunit exchange between two homoaggregates was also determined by FRET by mixing AIAS-labeled αB-wt with LYI-labeled αA-wt or αA-R116C in a 1:3 ratio at room temperature in the absence of GdnHCl. At room temperature, the fluorescence emission intensity remains unaltered since the donor and the acceptor are far apart. However, the fluorescence intensity was markedly altered at 37 °C. The time-dependent decrease in AIAS emission intensity at 426 nm and a concomitant increase in LYI fluorescence at 515 nm were indicative of energy transfer due to the proximity of the two fluorophores (Figure 8). After 2 h at 37 °C, there was no change in the emission intensity, implying achievement of stable equilibrium. We have calculated the rate of subunit exchange from the increase in acceptor fluorescence intensity (corrected). Figure 9 shows a plot of F_t/F_0 of LYI at 515 nm as a function of time, where F_t is the emission intensity at time t and F_0 is that at time zero. The increased emission intensity of LYI was divided by a factor 2 for αA-R116C since there are two LYI fluorophores per subunit. The rate constant was obtained by fitting the data to the exponential function $F_t/F_0 = A_1 + A_2e^{-kt}$, where A_1 and A_2 are constants and k is the rate constant for subunit exchange. The rates of subunit exchange were found to be 8.4×10^{-4} s^{-1} for αB-wt and αA-wt. Surprisingly, a nearly 3-fold higher rate constant (24.2×10^{-4} s^{-1}) was obtained for αB-wt and αA-R116C than for αB-wt and αA-wt.

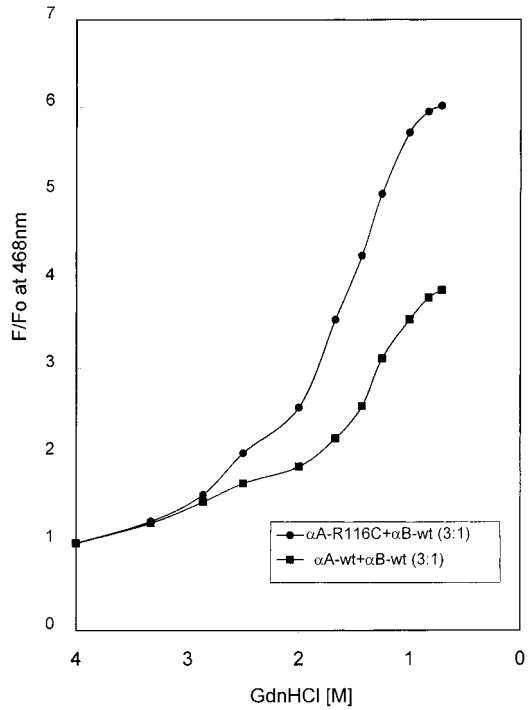

FIGURE 7: Denaturant concentration-dependent changes in emission intensity due to subunit exchange. The increase in relative fluorescence intensity at 468 nm due to fluorescence resonance energy transfer from PM-labeled αA-wt or αA-R116C crystallin to DMACA-labeled αB-wt crystallin. Fluorescently labeled αA-wt or αA-R116C crystallin was mixed with fluorescently labeled αB-wt crystallin in a 3:1 ratio with a final protein concentration of 1 mg/mL, and 4 M GdnHCl. After each dilution of the mixture was thoroughly mixed and left to incubate for 10 min, the fluorescence intensity was then measured and the readings were corrected for dilution. The increase in intensity was plotted vs GdnHCl concentration.

Chaperone-like Activity of the Reconstituted α-Crystallins. The chaperone-like activity of reconstituted α-crystallins was studied by monitoring the ability of this protein to prevent the denaturation and aggregation of ADH at 37 °C at two different proportions (1:2 and 1:10 α-crystallin:ADH) of reconstituted α-crystallin. Figure 10 shows a different degree of protection against aggregation by reconstituted α-crystallins. The protective ability of reconstituted α-crystallin from αA-wt and αB-wt was always greater than that from αA-R116C and αB-wt. Approximately 30 and 10% losses of chaperone-like activity were observed for 1:10 and 1:2 proportions, respectively, for reconstituted αA-R116C and αB-wt when compared to that with reconstituted αA-wt and αB-wt.

DISCUSSION

In 1992, it was shown that lens α-crystallin (heteroaggregates of αA and αB subunits) has chaperone-like properties (*5*). Also, now it is well established that individual homoaggregates of αA or αB can function as chaperones. In general, it is accepted that α-crystallin exists as heteroaggregates of αA and αB subunits in the lens, though Bhat et al. (*23*) concluded that αB-crystallin may exist as an independent protein not only in non-lens tissues but also in the lens. The stabilization of αB by αA was recently demonstrated by a study of αA-knockout mice (*24*). Mice with the targeted disruption of the αA gene developed lens

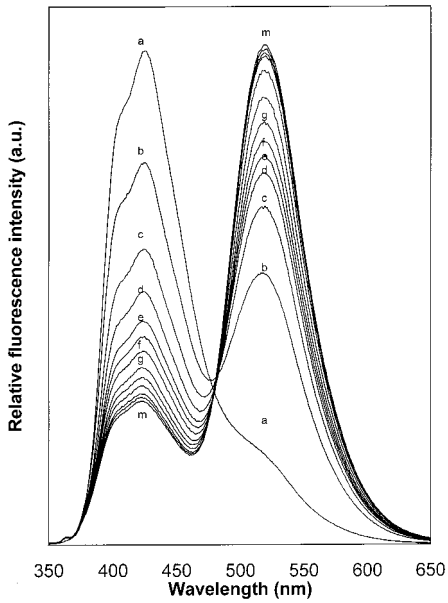

FIGURE 8: Time-dependent FRET due to subunit exchange of AIAS-labeled αB-crystallin and LYI-labeled αA-R116C crystallin. The emission spectra of αB-crystallin excited at 336 nm were recorded 0 (a), 2 (b), 4 (c), 6 (d), 8 (e), 10 (f), 15 (g), 25 (h), 45 (i), 75 (j), 120 (k), 180 (l), and 240 min (m) after mixing of LYI-labeled αA-R116C crystallin and AIAS-labeled αB-crystallin in a 3:1 ratio, with a final protein concentration 1 mg/mL. The decrease in fluorescence intensity at 426 nm of the AIAS-labeled protein and the concomitant increase in fluorescence intensity at 515 nm of the LYI-labeled protein are indicative of energy transfer due to exchange of subunits between the two labeled populations.

opacification starting from the nucleus and showed dense inclusion bodies that contain mostly αB. It appears that the heteroaggregate form of α-crystallin is essential in the lens (in vivo) for maintaining lens transparency. Therefore, it is important to show the mode of interactions between these two subunits and the structure−function properties of the reconstituted α-crystallin from αA- and αB-crystallin and to show whether the R116C mutation in αA-crystallin affects subunit interactions as well as structure−function properties. Previously, we reported that the homoaggregates of the mutant αA-R116C, known to be one of the causes of autosomal dominant congenital cataract, has modified structure with less chaperone activity (*15*). This investigation gives answers to basically two questions: first, as we believed that α-crystallin exists in the form of heteroaggregates in the lens, how αA-wt and αA-R116C interact with αB-crystallin to form α-crystallin; and second, whether the structural and functional properties of reconstituted α-crystallin from αA-R116C and αB-crystallin differ from those of α-crystallin from αA-wt and αB-crystallin. To answer these questions, we reconstituted α-crystallin from αA-wt and αB-crystallin as well as from αA-R116C and αB-crystallins in the two αA:αB ratios (1:1 and 3:1) because these are extreme ratios found in α-crystallin depending on age (*4*).

The most noteworthy effect of mutation of R116 to C may be considered to be the alteration of the subunit composition as well as enhancement of the size of heteroaggregates generated from the mutated αA-crystallin and αB-wt mixed in a 3:1 ratio. The subunit composition and the ratio of the mutant heteroaggregate was found to be 3:2.4 (∼1:1) rather than 3:1. The heteroaggregate size was almost twice that formed from their wild-type counterparts under similar

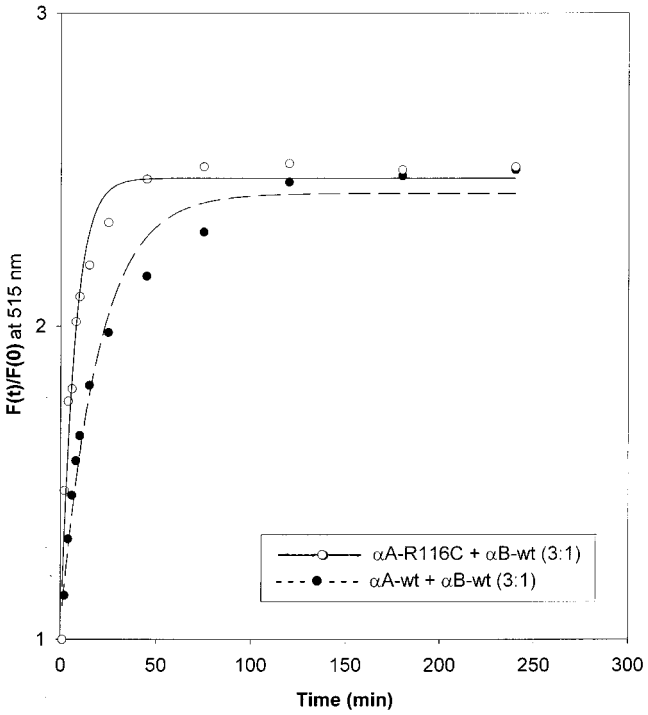

FIGURE 9: Time-dependent increase in emission intensity due to subunit exchange. Increase in the relative fluorescence intensity at 515 nm due to fluorescence resonance energy transfer from the AIAS-labeled protein to the LYI-labeled protein. AIAS-labeled αB-wt crystallin was incubated with LYI-labeled αA-wt and αA-R116C. Each curve represents the best statistical fit of the data to the exponential function $F_t/F_0 = C_1 + C_2e^{-kt}$. The rate constants determined by curve fitting were 8.4×10^{-4} and 24.2×10^{-4} s^{-1} for αB-wt with αA-wt and αB-wt with αA-R116C, respectively.

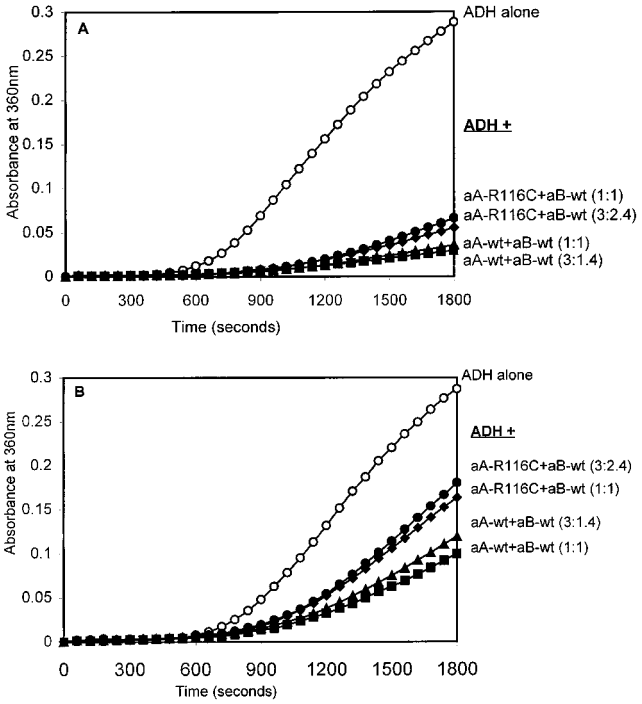

FIGURE 10: Chaperone-like activity of reconstituted α-crystallins. EDTA induced aggregation of 0.4 mg/mL ADH alone and in the presence of 0.2 mg/mL [1:2 chaperone:ADH ratio (A)] and 0.04 mg/ml [1:10 chaperone:ADH ratio (B)] reconstituted α-crystallin.

conditions. The tendency to form larger oligomers of ~2000 kDa has also been noted with the mutant homoaggregates (*15*). The effect of inclusion of αB-crystallin within the aggregate was found to reduce the size to a considerable extent (Figure 1).

As a result of the mutation of R116 to C in αA-crystallin, the subunit suffers a loss of 1 unit of positive charge at physiological pH compared to its wild-type counterpart. Also, it has been observed in this work (see later) that upon mutation the subunit suffers a considerable loss of surface hydrophobicity. The size of the soluble aggregate is generally determined by a delicate balance of the charge and hydrophobic interactions. It has been reported (*25*) that successive removal of residues from the highly charged C-terminal end of αA-crystallin produces successively larger aggregates. R116 is known to be located near the subunit interface and hence is likely to take part in subunit−subunit interactions (*26*). It has been reported (*27*) with many heat-shock proteins that if amino acid side chains involving subunit contacts for forming oligomeric aggregates are changed, the size and symmetry of the oligomers are found to vary. The stability of larger aggregates is generally attained by the burial of hydrophobic surfaces in the increased total internal volume of the aggregates, leaving very little hydrophobicity on the surface of the aggregates, inconsistent with the observation made in this work.

The fluorescence labeling experiment with the wild-type and mutant αA subunit (Figure 8) confirms the rationale that the subunits do interact to form the heteroaggregates. The validity of the dissociation−reassociation procedure used in this work for reconstitution of heteroaggregates has also been affirmed by the results of FRET experiments (Figure 7), where with the decrease in denaturant concentration, the fluorescence emission intensity of the acceptor molecule (αB-wt crystallin) at 460 nm, is found to be increased at the cost of that of the donor molecule (αA-wt/mutant), an indication of their interactions in forming the heteroaggregate. The rate of subunit exchange as obtained from Figure 9 between the mutant αA homoaggregate and the αB-wt homoaggregate has been found to be quite high when compared with that between the αA-wt homoaggregate and the αB-wt homoaggregate. The rate constant in the case of mutant subunit exchange (24.2×10^{-4} s^{-1}) has been found to almost 3 times greater than that with wild-type subunit exchange (8.4×10^{-4} s^{-1}). With the loss of 1 unit of positive charge, the mutant subunit assumes a somewhat lower isoelectric point and hence its net surface charge would be more negative under physiological conditions than that of its wild-type counterpart. With the net surface charge of αB-wt crystallin being positive under this condition, the electrostatic attraction of the mutant αA-crystallin toward αB will be somewhat stronger than that of αA-wt crystallin. The very first step of subunit−subunit interaction is generally considered to be Columbic interactions between the subunits followed by other noncovalent interactions for the subsequent stabilization of the oligomeric aggregates. The enhanced rate of exchange for the mutant αA subunit compared to that for the wild type may be suggested to be partly because of its stronger electrostatic interaction toward αB-crystallin. The 4-fold reduced ability (*28*) of the mutant αA-crystallin to exchange subunits with the αA-wt homoaggregate supports this view. The increased surface area of the mutant homoaggregates (twice that of wild-type homoaggregates) may also be a reason for the observed increased exchange rate. The high

rate of subunit exchange between αA-R116C and αB-wt does not appear to be due to extra Cys residue in αA-R116C. This conclusion is strengthened by the observation that the rate of subunit exchange (data not given) between αA-R119C having normal structure and function (*29*, *30*) and αB-wt is the same as that between αA-wt and αB-wt.

The extent of binding of the hydrophobic fluorophore, TNS, to any protein is customarily considered to be a measure of the available hydrophobic surface on the protein. Because of this, the available hydrophobic surface on the mutant αA-crystallin has been found to be considerably smaller when compared to that of αA-wt crystallin (*15*). In this work, it has been demonstrated (Figure 5) that the hydrophobic surface available on the mutant heteroaggregate remains almost unchanged, if not further decreased to an extent of ∼10%. It has already been indicated earlier (*15*, *16*) that merely a point mutation of Arg to Cys in αA-crystallin by itself is not expected to reduce the available hydrophobic surface area on the subunit homoaggregate to such an extent unless there is a change in the conformation of the subunit because of mutation. The further change in conformation that accompanies the inclusion of the αB-wt subunit during the formation of the heteroaggregate does not favor the exposure of hydrophobic surface. The hydrophobic surfaces reside all within the internal core of the heteroaggregate.

It is well-known that the Trp fluorescence emission maximum in a protein is an index of the extent of exposure of Trp side chains in this protein toward solvent (*31*, *32*). A complete exposure of Trp in a protein would generally exhibit the emission maximum at around 350 nm which is the emission maximum of free Trp in solution. The more this value is blue shifted, the more Trp side chains in the protein are considered to be less exposed to the solvent, i.e., buried in its inner core. This value has been found to be 337 nm for both the mutated and wt-αA homoaggregates (*15*) as well as for heteroaggregates of the αA mutant and αB-wt (Figure 4) at room temperature, indicating that Trp side chains in all these aggregates are buried almost to the same extent in the hydrophobic core. However, with the increase in temperature from 30 °C, the extent of exposure of Trp side chains to solvent has been found to increase to some extent within the mutant heteroaggregates in contrast to wild-type heteroaggregates. This is evidenced from the gradual red shifting of the Trp emission maximum which levels off at ∼340 nm at 40 °C. A thermally induced conformational change has been reported at around the same temperature with native α-crystallin (*33*), but this phenomenon has been found to accompany a considerable increase in surface hydrophobicity, exhibiting maximum chaperone activity at this temperature. For this reason, chaperone activity, in fact, is routinely measured at 37 °C rather than at room temperature. In the case of mutant heteroaggregates, this conformational change does not appear to result in any increase in surface hydrophobicity except the Trp side chains being more solvent exposed. This indicates that the Trp microenvironment in the mutant heteroaggregate is different from that in the wild-type heteroaggregate in the sense that the former is more thermally sensitive.

The far-UV CD spectra for the mutant heteroaggregates when compared with those for the wild-type heteroaggregates indicate that there is not much change in the backbone conformation of the subunits. The unfolded subunits have regained their proper backbone conformation despite the point mutation. This is affirmed by the unaltered minima at 216 nm and the identical crossover point at 204 nm for both spectra (Figure 2). The near-UV CD spectra of a protein are generally believed to offer an insight into the so-called tertiary structure of a protein (more precisely, the aromatic environments in the tertiary structure) formed by folding of secondary structural elements as well as by their subsequent packing to form a compact three-dimensional structure. Since α-crystallin subunits are highly aggregating in nature, it is not possible to think of tertiary structure of a single subunit. Instead, the near-UV CD spectra of α-crystallins exhibit the tertiary structure of subunits that has already suffered a perturbation (if any) (*34*) because of the homologous and/or heterologous subunit packing during the formation of homo- and heteroaggregates. The near-UV CD spectrum of αA-wt homoaggregates is distinctly different from that of αB-wt homoaggregates (Figure 3). This difference may be attributed to the difference in the tertiary structure of the individual subunit and/or to the difference of the effect of homologous subunit packing (between αA−αA and αB−αB pairs) upon their tertiary structure. The αA-wt profile is characterized by five distinctly defined maxima around 259, 265, 273, 279, and 287 nm and five distinct minima around 262, 268, 275, 284, and 292 nm. The negative vibronic signals at 292 and 284 nm minima are due to Trp residues (*35*). The maxima at 259 and 265 nm and the minima at 268 and 262 nm are characteristics of Phe fine structure. The remaining transitions between 270 and 280 nm arise from Tyr and/or Trp, 287 nm maxima being considered to be due to Tyr residue. On the contrary, in the αB-wt profile except for the two sharply defined maxima at 259 and 265 nm and the two sharply defined minima at 262 and 268 nm, those in the spectral region beyond 270 nm are only recognizable but not sharply defined as in the αA-wt profile. The ellipticity values corresponding to these maxima are also found to be widely different for the two wild-type homoaggregates. In the profile of mutant homoaggregates, except the Phe fine structure which is found to be retained, the entire spectral region beyond 270 nm is practically structureless. This shows that the mode of folding of the secondary structural elements in forming the tertiary structure as well as the effect of homologous packing of the mutant subunit upon the tertiary structure is distinctly different from those in the wild-type homoaggregates. The differences may be attributed mainly to the alterations in the interaction of aromatic (Tyr and Trp) chromophores in the mutant homoaggregates. This is not unlikely, since the replacement of the bulky side chain of Arg with a comparatively smaller one of Cys is not isosteric in nature and hence must affect the packing mode of subunits in space during homoaggregation.

Upon inclusion of the αB-wt crystallin, the reconstituted mutant heteroaggregate regained to some extent the fine structure in the spectral region from 270 nm onward. Thus, the maxima at 273, 279, and 287 nm have been found to be re-formed together with the characteristic negative vibronic signal of the Trp transition around 292 nm which appears to be a positive vibronic signal in the mutant homoaggregate. However, the spectra still appear to be much less structured in the Tyr/Trp region compared with the profile of the wild-type heteroaggregates. This somewhat loosely packed struc-

ture of the mutant heteroaggregates particularly in the Tyr/Trp microenvironments may be responsible for its thermal sensitivity toward Trp exposure observed in our fluorescence studies (Figure 4). Interestingly, the near-UV CD profile of the mutant heteroaggregates more closely resembles the profile of the αB-wt homoaggregates, whereas the profile of the wild-type heteroaggregates more closely resembles that of the αA-wt homoaggregates. This can be explained by the predominance of αA-wt crystallin in the wild-type heteroaggregates and that of αB-wt crystallin in the mutant heteroaggregates, thus supporting the difference in subunit composition in mutant heteroaggregates compared to that of wild-type heteroaggregates discussed earlier in this work.

Arg-116 is a highly conserved residue in the entire heat-shock family of proteins and in 28 species of mammals and other vertebrates (*36*). This work shows that mutation of this Arg to Cys leads to less compact heteroaggregates that are much larger. These high-molecular weight aggregates may cause problems of scattering and/or insolubility as well as improved ability to bind the membrane (*30*). However, if indeed, the mutant αA-R116C exists as heteroaggregates in the human lens, a reduction of ∼10% in chaperone activity at a physiologically relevant α-crystallin to target protein ratio may not be the leading factor in the congenital cataract formation which is well-known for this particular mutation. On the other hand, if it is present predominantly as homo-aggregates in the lens, an ∼40% reduction in chaperone activity (*15*) will be significant.

REFERENCES

1. Van Der Ouderaa, F. J., De Jong, W. W., Hilderink, A., and Bloemendal, H. (1974) *Eur. J. Biochem. 49*, 157−168.
2. Bloemendal, H. e. (1981) *Molecular and Celluar Biology of the Eye Lens*, pp 1−47, John Wiley & Sons, New York.
3. Derham, B. K., and Harding, J. J. (1999) *Prog. Retinal Eye Res. 18*, 463−509.
4. Swamy, M. S., and Abraham, E. C. (1991) *Curr. Eye Res. 10*, 213−220.
5. Horwitz, J. (1992) *Proc. Natl. Acad. Sci. U.S.A. 89*, 10449−10453.
6. Bhat, S. P., and Nagineni, C. N. (1989) *Biochem. Biophys. Res. Commun. 158*, 319−325.
7. Dubin, R. A., Wawrousek, E. F., and Piatigorsky, J. (1989) *Mol. Cell. Biol. 9*, 1083−1091.
8. Iwaki, T., Kume-Iwaki, A., Liem, R. K., and Goldman, J. E. (1989) *Cell 57*, 71−78.
9. Kato, K., Shinohara, H., Kurobe, N., Goto, S., Inaguma, Y., and Ohshima, K. (1991) *Biochim. Biophys. Acta 1080*, 173−180.
10. Lowe, J., Landon, M., Pike, I., Spendlove, I., McDermott, H., and Mayer, R. J. (1990) *Lancet 336*, 515−516.
11. Renkawek, K., de Jong, W. W., Merck, K. B., Frenken, C. W., van Workum, F. P., and Bosman, G. J. (1992) *Acta Neuropathol. 83*, 324−327.
12. Head, M. W., Corbin, E., and Goldman, J. E. (1993) *Am. J. Pathol. 143*, 1743−1753.
13. Vicart, P., Caron, A., Guicheney, P., Li, Z., Prevost, M. C., Faure, A., Chateau, D., Chapon, F., Tome, F., Dupret, J. M., Paulin, D., and Fardeau, M. (1998) *Nat. Genet. 20*, 92−95.
14. Litt, M., Kramer, P., LaMorticella, D. M., Murphey, W., Lovrien, E. W., and Weleber, R. G. (1998) *Hum. Mol. Genet. 7*, 471−474.
15. Shroff, N. P., Cherian-Shaw, M., Bera, S., and Abraham, E. C. (2000) *Biochemistry 39*, 1420−1426.
16. Kumar, L. V., Ramakrishna, T., and Rao, C. M. (1999) *J. Biol. Chem. 274*, 24137−24141.
17. Shroff, N. P., Cherian, M., and Abraham, E. C. (1998) *Invest. Ophthalmol. Visual Sci. 39*, S1018.
18. Shroff, N. P. (1999) Ph.D. Thesis, Medical College of Georgia, Augusta, GA.
19. Laemmli, U. K. (1970) *Nature 227*, 680−685.
20. Brazil, B. T., Ybarra, J., and Horowitz, P. M. (1998) *J. Biol. Chem. 273*, 3257−3263.
21. Smith, S. P., Barber, K. R., Dunn, S. D., and Shaw, G. S. (1996) *Biochemistry 35*, 8805−8814.
22. Siezen, R. J., and Bindels, J. G. U. (1982) *Exp. Eye Res. 34*, 969−983.
23. Bhat, S. P., Horwitz, J., Srinivasan, A., and Ding, L. (1991) *Eur. J. Biochem. 202*, 775−781.
24. Brady, J. P., Garland, D., Duglas-Tabor, Y., Robison, W. G., Jr., Groome, A., and Wawrousek, E. F. (1997) *Proc. Natl. Acad. Sci. U.S.A. 94*, 884−889.
25. Siezen, R. J., Bindels, J. G., and Hoenders, H. J. (1979) *Exp. Eye Res. 28*, 551−567.
26. Berengian, A. R., Bova, M. P., and McHaourab, H. S. (1997) *Biochemistry 36*, 9951−9957.
27. Kim, K. K., Kim, R., and Kim, S. H. (1998) *Nature 394*, 595−599.
28. Cobb, B. A., and Petrash, J. M. (2000) *Biochemistry 39*, 15791−15798.
29. Bera, S., Shroff, N. P., and Abraham, E. C. (2000) *Invest. Ophthalmol. Visual Sci. 41*, S583.
30. Cherian-Shaw, M., Shroff, N. P., and Abraham, E. C. (2000) *Invest. Ophthalmol. Visual Sci. 41*, S749.
31. Kronman, M. J., and Holmes, L. G. (1971) *Photochem. Photobiol. 14*, 113−134.
32. Burstein, E. A., Vedenkina, N. S., and Ivkova, M. N. (1973) *Photochem. Photobiol. 18*, 263−279.
33. Ramon, B., Ramakrishna, T., and Rao, Ch. M. (1995) *FEBS Lett. 365*, 133−136.
34. Datta, S. A., and Rao, Ch. M. (2000) *J. Biol. Chem. 275*, 41004−41010.
35. Strickland, E. H. (1974) *Crit. Rev. Biochem. 2*, 113−175.
36. de Jong, W. W., Zweers, A., Versteeg, M., and Nuy-Terwindt, E. C. (1984) *Eur. J. Biochem. 141*, 131−140.

BI011010V